ELSEVIER

15 September 1995

Optics Communications 119 (1995) 597–603

OPTICS COMMUNICATIONS

Anisotropic strong volume hologram in $BaTiO_3$

Ching-Cherng Sun [a], Ming-Wen Chang [b], Ken Yuh Hsu [c]

[a] *Optical Sciences Center, National Central University, Chung-Li 32054, Taiwan, ROC*

[b] *Institute of Optical Sciences, National Central University, Chung-Li 32054, Taiwan, ROC*

[c] *Institute of Electro-Optical Engineering, National Chiao Tung University, Hsinchu, Taiwan, ROC*

Received 13 March 1995

Abstract

A photorefractive strong volume hologram by using anisotropic diffraction in a normal-cut $BaTiO_3$ is proposed and demonstrated. Experimental measurements fit the theoretical calculations well by using Kogelnik's formula with unclamped E-O coefficients. The maximum refractive index perturbation in the experiment is larger than 2.7×10^{-4}. In addition, we have observed that the output of the diffracted light are concentric circles. This pattern is shown as a good guide of the estimation of how large the refractive index perturbation is. The Bragg condition of the anisotropic strong volume hologram is so strict that an image-carried hologram cannot be directly read out. We proposed an address image method by erasure for solving this problem. Through this method, this anisotropic strong volume hologram has some potential for optical image storage.

1. Introduction

Photorefractive crystals have been extensively studied for their potential applications of optical storage and real-time information processing which include optical correlation, phase conjugation, optical computing and interconnections [1–4]. Inside a photorefractive crystal, holograms would have different characteristics for different writing conditions which induce different applications. In the steady state, the diffraction efficiency of a photorefractive grating can be treated as a fixed volume hologram that is described by Kogelnik's formula [5],

$$\eta=\sin^2\left(\frac{\pi\Delta n d}{\lambda\cos\theta}\right)\exp\left(-\frac{\alpha d}{\cos\theta}\right). \tag{1}$$

Where Δn is the amplitude of the refractive index change, d is the thickness of the hologram, θ is the incident angle of the probe beam inside the crystal, λ is its wavelength and α is the absorption coefficient. Eq. (1) shows that the diffraction efficiency is a periodic function of the coupling parameter which is the product of the refractive index change and the interaction length. When the incident lights interfere inside a photorefractive crystal, the photo-excited charges are redistributed through the diffusion and/or drift processes. Then the space charge field is built and it leads to a refractive index change through the Pockels effect (simplified as E-O effect) [6]. The amplitude of the refractive index perturbation is [7]

$$\Delta n=-\tfrac{1}{2}n^3\gamma_{\mathrm{eff}}mE_{\mathrm{sc}}, \tag{2}$$

where Δn is the amplitude of index perturbation, m is the light modulation depth, n is the background refractive index, γ_{eff} is the effective E-O coefficient and E_{sc} is the amplitude of the space charge field. In $BaTiO_3$, the diffusion field is dominant for the construction of space charge field and can be expressed as [8]

$$E_{\mathrm{sc}}=\frac{K_{\mathrm{B}}T}{q}\frac{K_{\mathrm{g}}}{1+(K_{\mathrm{g}}/K_{\mathrm{o}})^2}, \tag{3}$$

SSDI 0030-4018(95)00372-X

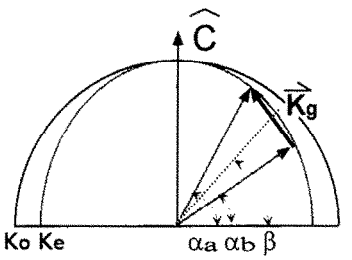

Fig. 1. The wave vector diagram of the diffraction in $BaTiO_3$ of which the optic axis lies on the incident plane.

where

$$K_o = \left(\frac{Nq^2}{\epsilon\epsilon_o K_B T}\right)^{1/2} . \tag{4}$$

K_B is Boltzmann's constant, T is the temperature, $q = 1.6\times10^{-19}$ C, N is the effective trap density, ϵ_o is the dielectric constant in the direction of the grating vector and K_g is the amplitude of the grating vector. Eq. (2) shows that Δn depends on the space charge field, the modulation depth and the effective E-O coefficient. Therefore, a crystal such as $BaTiO_3$ which has a large effective E-O coefficient may be constructed for a high diffraction efficiency. In general, when the optic axis lies on the incident plane, and an extraordinarily polarized beam is used as the reading beam, the effective E-O coefficient can be expressed as [9]

$$\gamma_{eff} = \frac{\cos\beta}{n_e n^3 \cos\alpha_a}\,(n_o^4\gamma_{13}\sin\alpha_a \sin\alpha_b + 2n_o^2 n_e^2\gamma_{42}\sin^2\beta + n_e^4\gamma_{33}\cos\alpha_a\cos\alpha_b) , \tag{5}$$

as shown in Fig. 1, where α_a, α_b and β are the angles of the reading beam, diffraction beam and the grating vector inside the crystal, respectively. All the angles are with respect to the normal of the optic axis. n_o, n_e are the refractive indices of ordinarily and extraordinarily polarized beams. γ_{13}, γ_{33} and γ_{42} are the nonzero E-O elements of $BaTiO_3$ and γ_{42} is the largest one. Fig. 2 shows a theoretical calculation of Δn as a function of both the full incident angles of the reading beams and the angle of the grating vector inside the crystal. The parameters for the calculations are $\gamma_{13} = 28$ pm/V, $\gamma_{33} = 80$ pm/V and $\gamma_{42} = 1640$ pm/V [8], $\epsilon_{=} = 105$, $\epsilon_{\perp} = 4300$, $n_o = 2.488$, $n_e = 2.424$ at $\lambda = 514.5$ nm [10], and $N = 2\times10^{16}$ cm^{-3} [8] while $T = 300$ K. As shown in Fig. 1, θ is the full incident angle. β and θ are defined as

$$\beta = \tfrac{1}{2}(\alpha_a + \alpha_b) , \tag{6}$$

$$\theta = \alpha_a - \alpha_b . \tag{7}$$

The maximum Δn can be found in the condition that the grating angle lies between 30° and 50° with small full incident angles between the incident beam and the diffracted beam [11]. In general, a normal-cut single crystal has difficulty in satisfying the required conditions. A strong volume hologram in which Δn reaches 1.67×10^{-4} has been reported in a 30°-cut $BaTiO_3$ for its large effective E-O coefficient [12]. In this paper, we demonstrated an anisotropic strong volume hologram (ASVH) in a normal-cut $BaTiO_3$ with the optic axis normal to the incident plane. Potential applications of this strong volume hologram will be proposed and discussed.

2. Anisotropic strong volume hologram

The wave vector diagram for anisotropic diffraction is shown in Fig. 3. As shown in the figure, the writing beams I_1 and I_2 are ordinarily polarized to avoid beam fanning and the wavelength is 514.5 nm. The reading beam is extraordinarily polarized and the wavelength is 633 nm. As a result, an ordinarily polarized beam I_d is diffracted under the Bragg condition. The effective grating vector has to satisfy the boundary condition for momentum conservation [13] as

$$k(n_o - n_e) \leqslant K_g \leqslant k(n_o + n_e) , \tag{8}$$

where k is the wave number in vacuum. There are two special characteristics of the anisotropic strong volume hologram. First, the coupling between the writing beams is forbidden due to the effective E-O coefficient being zero. Second, the polarizations of the reading beam and the diffracted beam are orthogonal so that no photorefractive grating is generated by them; besides, weak coupling through the photogalvanic effect can be neglected [14]. Therefore, only one dominant Bragg-matched grating exists in the hologram as shown in Fig. 3 and no other grating contributes to the coupling [15]. The effective E-O coefficient of anisotropic diffraction in $BaTiO_3$ is [16]

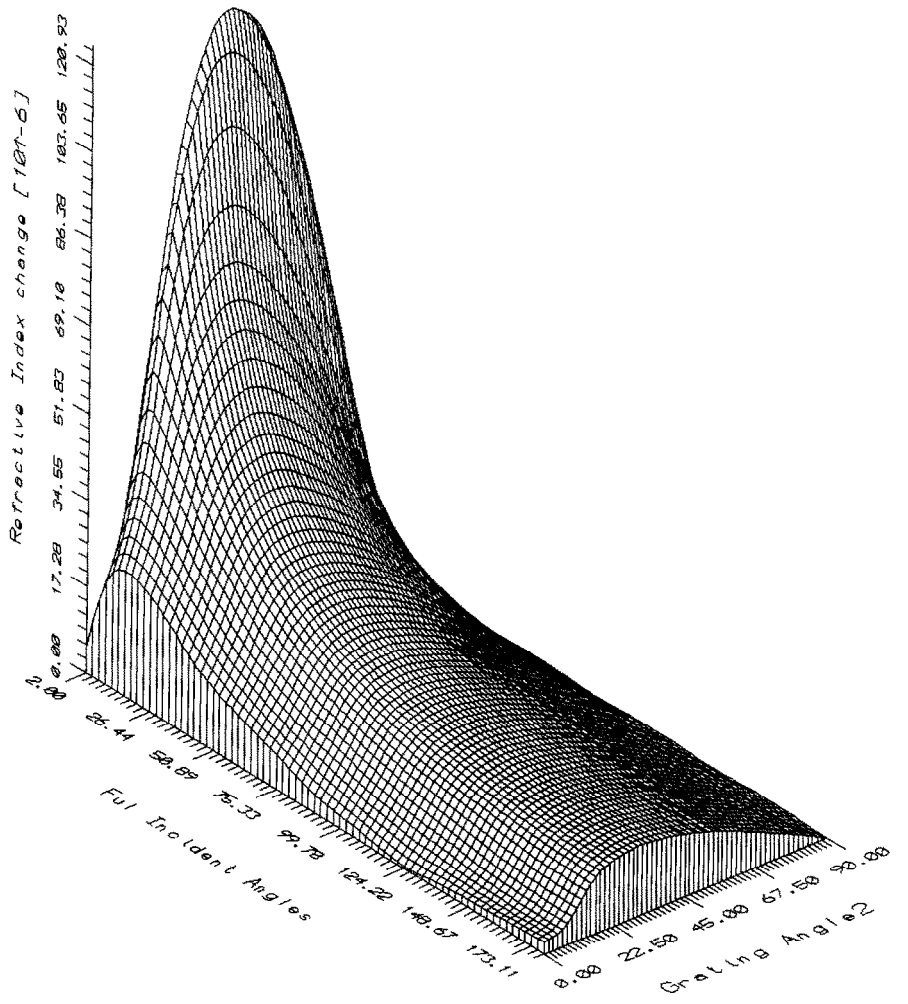

Fig. 2. Theoretical calculation of Δn as a function of Bragg-matched incident angles of the reading beam (incident angles 1) and the diffraction beam (incident angles 2) with an extraordinary polarization in $BaTiO_3$ of which the optic axis lies on the incident plane. The maximum Δn is obtained when the incident angles are 41° and 46°, respectively.

$$\gamma_{\text{eff}} = n_o n_e^2 \gamma_{42} / n^3 . \tag{9}$$

In Eq. (9), the effective E-O coefficient is independent on the reading angle. Fig. 4 shows the theoretical calculations of Δn and the corresponding diffraction efficiency with respect to the Bragg-matched reading angle by using Eqs. (1)–(4) and (9). The parameters for the calculations are $n_o = 2.42$ and $n_e = 2.36$ at $\lambda = 633$ nm [10]. The figure shows that both Δn and the corresponding diffraction efficiency are functions of the reading angles. This is because the space charge field depends on the amplitude of the grating vector as shown in Eq. (3). And as shown in Fig. 3, the special Bragg condition induces that each amplitude of the grating vector corresponds to a specific Bragg-matched reading angle.

3. The experiment and discussions

The schematic diagram of the experimental setup is shown in Fig. 5. Two writing beams were derived from

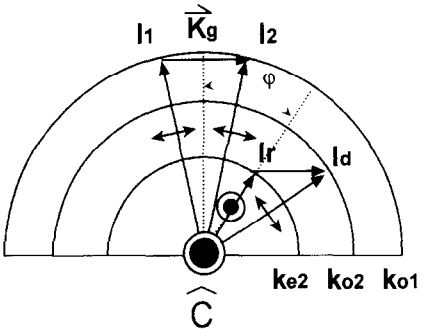

Fig. 3. The wave vector diagram of the anisotropic diffraction. K_g is the grating vector written by I_1 and I_2. I_r and I_d are the Bragg-matched writing beam and diffracted beam. K_{01}, K_{e2} and K_{02} are the wave numbers of the writing beam, reading beam and diffracted beam, respectively.

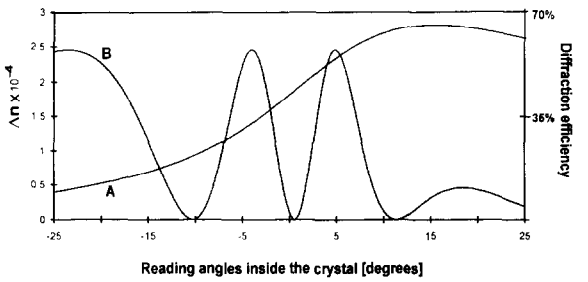

Fig. 4. Curve A: the theoretical calculation of Δn as a function of Bragg-matched reading angles inside the crystal. Curve B: the normalized diffraction efficiency corresponding to curve A with the crystal length 6.6 mm.

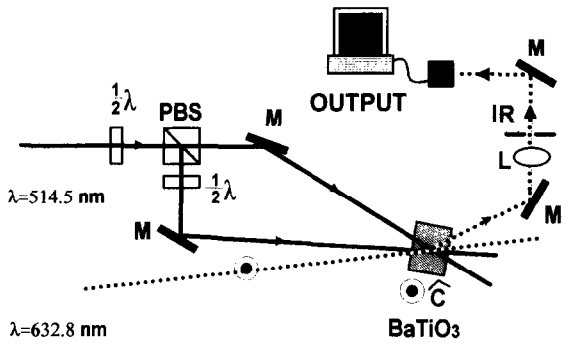

Fig. 5. The schematic diagram of the experimental setup, where $\frac{1}{2}\lambda$ is the half wave plate, PBS the polarized beam splitter, M the mirror, L the lens and IR the iris.

an Innova 90-5 argon-ion laser with TEM_{00} at $\lambda = 514.5$ nm in ordinary polarization. The reading beam was derived from an HeNe laser in extraordinary polarization. The total intensities of the writing beams were 700 mW/cm^2, and the reading beam was 5 mW/cm^2. The dimension of the crystal was $6.6\times6.6\times7$ mm^3 ($a\times b\times c$). The incident angle of the reading beam was Bragg-matched by adjusting the micropositioner of the mirror to reach the maximum diffraction efficiency under small modulation depths ($m \ll 1$). Then the beam ratio was adjusted to 1 : 1. It can be observed that the output pattern consisted of concentric circles as shown in Fig. 6. This pattern was caused by different effective grating thicknesses for different parts of the reading beam. The diameter of the writing beams are both 2.5 mm. They cannot cover the whole crystal and the grating in a rhomb-like region along the crystal. In the experiment, only the central portion of the reading beam is adjusted to read the thickest portion of the grating. Therefore the central portion of the diffraction beam gets the largest coupling strength. In contrast, the outer portion of the diffraction pattern corresponds to the shorter grating thickness and the smaller coupling strength. Thus the concentric circles can be easily understood when we apply Eq. (1). If the coupling strength $\Delta n\, d$ is large enough such that the argument reaches several times the period of the $\sin^2$ function, a decrease of $\Delta n\, d$ from the central part to the outer part will induce a corresponding intensity oscillation of the

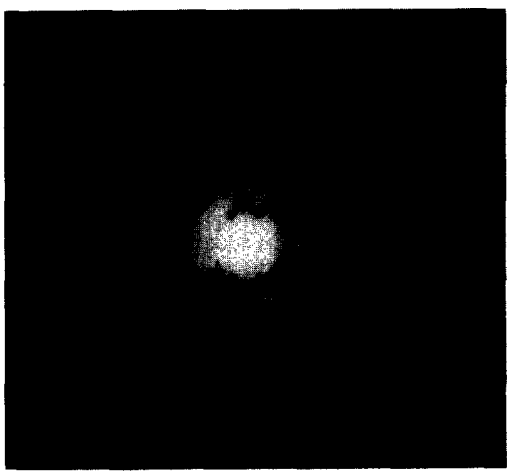

Fig. 6. The output of the diffraction light are concentric circles.

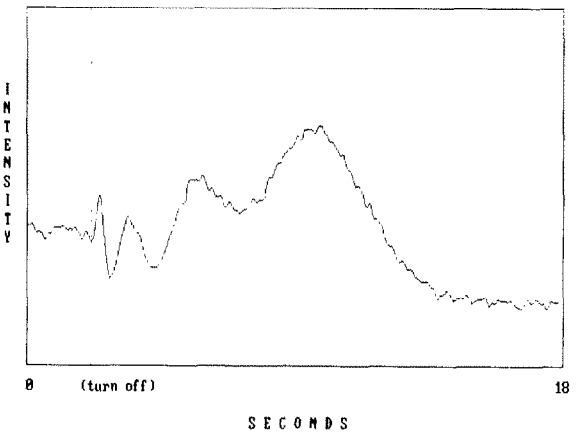

Fig. 7. The temporal behavior of the diffraction efficiency when the reading angle inside the crystal is 8.1°. The oscillation is caused by the decay fo the grating strength. The intensity of the reading beam is 5 mW/cm^2.

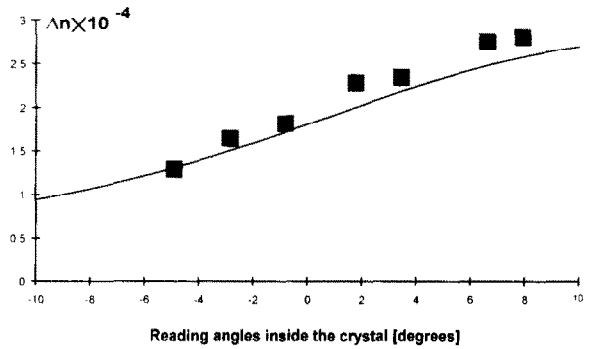

Fig. 8. Experimental measurements of Δn vs. the Bragg-matched reading angles. The solid line gives the corresponding theoretical calculations.

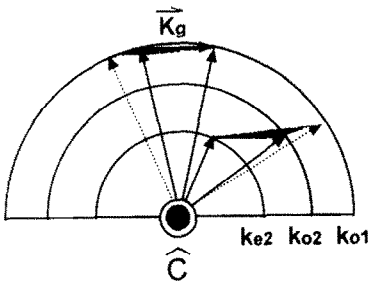

Fig. 9. The wave vector diagram of the anisotropic diffraction. The image-carried gratings cannot be read out by a plane wave because all the Bragg conditions cannot be fully satisfied at the same time.

diffraction pattern. Therefore, the number of concentric circles can show how large Δnd was in the experiment. It is interesting that the concentric circle offers a guide of how large the refractive index perturbation was. Because only the central part of the output pattern was needed for measuring the maximum Δn, an iris was used to block the outer portion of the output. After the grating had reached a steady state, the writing beams were turned off abruptly, and the grating was erased by the reading beam. According to Eq. (1), the diffraction intensity will oscillate as the grating decays. The temporal behavior o the diffraction efficiency was recorded and shown in Fig. 7. In the figure the number of oscillations in the diffraction efficiency can be used to calculate the corresponding Δn by using Eq. (1), and Δn can be obtained in the experiment. Fig. 7 shows the theoretical calculations of Δn corresponding to the experimental measurements. It is seen from the figure that the experimental results fit the theoretical calculations well by using the unclamped parameters. The maximum refractive index perturbation is larger than 2.7×10^{-4}. Two conclusions from the above experimental measurements are discussed in the following. First, Fig. 8 shows that the diffraction efficiency of the photorefractive grating can be well predicted by using Kogelnik's formula. This is caused by the inhibition of the coupling between two writing beams. On the other hand, the diffracted and reading beams do not generate another dominant grating. Therefore, it can be said that only one grating exists. This is different from most conditions in the photorefractive crystal. Second, the experimental data show that such an operation is in an unclamped condition.

4. The potential application

After the discovery of fixing holograms in $BaTiO_3$ [17], $BaTiO_3$ has some potential for optical data storage because of its large refractive index perturbation. It may allow a high storage capacity [12]. We have shown that ASVHs indeed exist when the optic axis is normal to the incident plane. Therefore, it is possible to use the ASVH as a high optical storage capacity device. But the strict Bragg condition makes it difficult to read out the information from the hologram. It is easy to see from Fig. 9 that a plane-wave reading beam cannot fully satisfy all the Bragg conditions of an

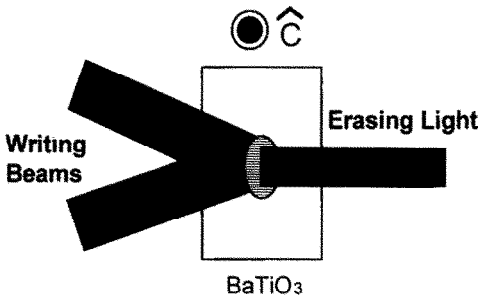

Fig. 10. The principle of the EMHA method. The image hologram is not written directly but is erased by using an incoherent image-carried light. The nonerasing portion keeps the unit grating vector and can be read out. The output will be the replica of the incoherent input image.

image-carrying volume hologram at the same time. To solve this problem, we proposed here an erasing-mode hologram address (simplified EMHA) method which is shown in Fig. 10. In the MAHA method, the information is not carried by the writing beams. In contrast, an image-coded light is used to erase the grating which is written by two incident beams without carrying any image. The nonerasure part of the grating keeps the unit grating vector and the erased grating can be read out by a plane wave. In general, the diffraction light has a negative replica of the input image. The EMHA method is very similar to the method used for the photorefrative incoherent-to-coherent optical converter (PICOC), but here EMHA is used for optical storage instead of optical conversion. In comparison with each other, the architectures are similar but the principles are different. In the case of a high capacity optical storage, multiple exposure must make the final diffraction efficiency to be always below the first peak of Eq. (1). The read-out pattern is always a negative replica of the input image. It is different when a strong volume hologram is used: the output image may be a negative or positive replica of the input image [18]. It depends on how large the refractive index perturbation is. Fig. 11 shows an output image which is operated when the diffraction efficiency of the writing grating is within the first highest and the first lowest ones. The image is therefore stored inside the crystal in a positive replica of the input image.

5. Conclusions

We have proposed and demonstrated an anisotropic strong volume hologram. In the experiments, a refrac-

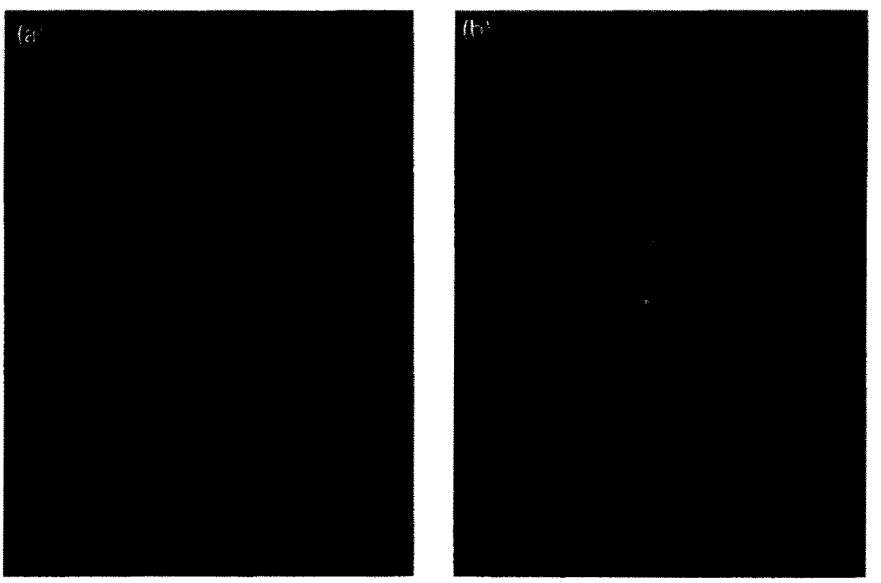

Fig. 11. (a) The image is stored inside the crystal. (b) The read-out image is a positive replica of the input image by operating the strength of the hologram so that the diffraction efficiency is between the first maximum and minimum.

tive index perturbation of more than 2.7×10^{-7} was observed in a 6.6 mm thick normal-cut $BaTiO_3$. The output light consisted of concentric circles, which was shown as a good guide for estimating how large the refractive index perturbation is. The measurements of the diffraction efficiency fitted well with the theoretical calculations with unclamped values of the E-O coefficients. On the other hand, for solving the strict Bragg condition of reading the hologram we have proposed an EMHA method. It is suitable especially for the application of optical storage in anisotropic diffraction.

Acknowledgements

This research was supported by the National Science Council of the Republic of China under contract NSC82-0417-E-008-097.

References

[1] F.H. Mok, M.C. Tackitt and H.M. Stoll, Optics Lett. 16 (1991) 605.
[2] P. Yeh, A.E. Chiou, P. Beckwith, T. Chang and M. Khoshnevisan, Opt. Eng. 28 (1989) 328.
[3] J.-P. Huignard and P. Gunter, Optical processing using wave mixing in photorefractive crystals, in: Photorefractive materials and their applications, Vol. II, eds. P. Gunter and J.-P. Huignard (Springer, New York, 1989) Ch. 6.
[4] Ching-Cherng Sun, Ming-Wen Chang and Ken Yuh Hsu, Appl. Optics 33 (1994) 4501.
[5] H. Kogelnik, Bell Syst. Tech. J. 48 (1969) 2909.
[6] N.V. Kukhtarev, V.B. Markov, S.G. Odulov, M.S. Soskin and V.L. Vinetskii, Ferroelectrics 22 (1979) 949.
[7] A. Yariv and P. Yeh, Optical waves in crystals (Wiley, New York, 1984) Ch. 7.
[8] K.R. MacDonald and J. Feinberg, J. Opt. Soc. Am. 73 (1983) 548.
[9] J. Feiberg and K.R. MacDonald, Photorefractive properties in $BaTiO_3$, in: Photorefractive materials and their applications, Vol. II, eds. P. Gunter and J.-P. Huignard (Springer, New York, 1989) pp. 156–160.
[10] S.H. Wemple, M. DiDomenico Jr. and I. Camilibel, J. Phys. Chem. Solids 29 (1968) 1797.
[11] Y. Fainman, E. Klancnik and S.H. Lee, Opt. Eng. 25 (1986) 228.
[12] J.H. Hong, P. Yeh, D. Psaltis and D. Brady, Optics Lett. 15 (1990) 344.
[13] P. Gunter and J.-P. Huignard, Photorefractive effecs and materials, in: Photorefractive materials and their applications, Vol. I, eds. P. Gunter and J.-P Huignard (Springer, New York, 1988) pp. 32–34.
[14] R.M. Pierce and R.S. Cudney, Optics Lett. 11 (1992) 784.
[15] D.A. Temple and C. Warde, J. Opt. Soc. Am. B 3 (1986) 337.
[16] N.V. Kukhtarev, E. Kratzig, H.C. Kulich and R.A. Rupp, Appl. Phys. B 35 (1984) 17.
[17] D. Kirillov and J. Feinberg, Optics Lett. 16 (1991) 1520.
[18] C.C. Sun, M.W. Chang and K.Y. Hsu, Optics Lett. 18 (1993) 655.